Experimental demonstration and stochastic modeling of autonomous formation of nanophotonic droplets

**Naoya Tate · Makoto Naruse · Yang Liu ·
Tadashi Kawazoe · Takashi Yatsui ·
Motoichi Ohtsu**

Abstract We have previously demonstrated a novel technique for autonomously forming a nanophotonic droplet, which is micro-scale spherical polymer structure that contains paired heterogeneous nanometric components. The sort-selectivity and alignment accuracy of the nanometric components in each nanophotonic droplet, and the related homogeneity of the optical function, are due to a characteristic pairing process based on a phonon-assisted photo-curing method. The proposed method requires irradiating a mixture of components with light to induce optical near-field interactions between each component, and subsequent processes based on these interactions. The pairing yield of components via the interactions is considered to mainly depend on the frequency of their encounters and the size-resonance effect between encountered components. In this paper, we model these two factors by individual stochastic procedures and construct a numerical model to describe the pairing process. Agreement between the results of numerical and experimental demonstrations shows the validity of our stochastic modeling.

1 Introduction

Nanophotonic devices utilize local interactions between nanometric components via dressed photon (DP), which

N. Tate (✉) · Y. Liu · T. Kawazoe · T. Yatsui · M. Ohtsu
The University of Tokyo, 2-11-16 Yayoi, Bunkyo-ku,
Tokyo 113-8656, Japan
e-mail: tate@nanophotonics.t.u-tokyo.ac.jp

M. Naruse
National Institute of Information and Communications
Technology, 4-2-1 Nukui-kita, Koganei, Tokyo 184-8795, Japan

have been proposed to meet the requirements of future optical technologies [1]. A DP is a quasi-particle representing the coupled state of a photon and an electron in a nanometric space [2]. DPs can excite multi-mode coherent phonons in the components during the interactions, and the DPs and phonons can electrically couple with each other [3–6]. The quasi-particle representing this coupled state has been named a dressed-photon–phonon (DPP). In particular, utilization of the energy transfer between semiconductor quantum dots (QDs) based on such interactions has been experimentally demonstrated, and novel functions and characteristic features have been realized [7–10]. One of the fundamental problems faced in using micro- and nano-scale physics to realize practicable nanophotonic devices and systems is the difficulty of establishing appropriate mechanisms for inducing the intended optical functions, which can be directly applied to macro-scale applications. At the same time, mass-production and uniform quality are also essential.

Self-assembly is one promising method of resolving such difficulties [11–14]. Also, several self-assembly methods for constructing nanophotonic devices have been developed [3,15–17]. Previously, the authors reported an autonomous technique for producing nanophotonic droplets [18]. A nanophotonic droplet is a micro-scale spherical structure that contains coupled QDs encapsulated by a locally cured photo-curable polymer. As has been experimentally verified [19], the produced nanophotonic droplets exhibit homogeneous sizes, shapes, and optical properties due to their autonomous formation process. During the process, a mixed solution of heterogeneous QDs and polymer is continuously irradiated with incident light having a lower photon energy than the activation energy of the polymer to induce DPP-mediated optical near-field interactions between the components and a subsequent phonon-assisted process [3–6]. The process

realizes multistep excitation via excited phonon levels, allowing the polymer to be cured by such low-photon-energy light. The essential point is that this process occurs only when heterogeneous QDs possess appropriate sizes, which has been called a size-resonance, and also electronic energy conditions.

The efficiency of the phonon-assisted process depends on the velocity-fluctuation of components in the mixed solution in addition to the size-resonance effect [20]. As theoretically reported in [20], the energy of the DPP-mediated optical near-field interactions between two nanometric structures is expected to be maximized when the sizes of the two components are similar. Because the phonon-assisted process for the coupling of QDs is fundamentally based on the DPP-mediated optical near-field interactions between the QDs, QDs with similar sizes are preferably coupled with each other due to the size-resonance effect. Therefore, if the sizes of the encountered QDs are quite similar so that they exhibit size-resonance, the phonon-assisted process is induced, and the encountered QDs are successfully coupled with each other.

In this paper, we focus on fluctuating behaviors of components in the mixed solution during the coupling process. In order to discuss fundamentals of the behaviors, we constructed a numerical model that consists of two individual stochastic procedures corresponding to the fluctuation and the size-resonance. Here, we considered thermal equilibrium state of the mixed solution in a finite temperature in which velocities of its components are distributed along Maxwell–Boltzmann distribution law. In such case, fluctuating behavior of each component is often simply described by using random walk model. First, we briefly review the basics of our phonon-assisted coupling process for forming a nanophotonic droplet. Then, we describe some experimental demonstrations. Finally, we propose a stochastic model of the coupling process and verify the validity of our model by comparison with the results of experimental demonstrations.

2 Basics of forming nanophotonic droplet

In our proposed method for producing nanophotonic droplets, a mixed solution of QDs and photo-curable polymer is illuminated by the light to generate DPP around each QD for fixing and coupling QDs by local-curing of the polymer via the phonon-assisted process based on DPP-mediated optical near-field interactions.

An overview of our proposed method is schematically shown in Fig. 1a. The sequence of forming a nanophotonic droplet is divided into two steps: coupling and encapsulating. We assume a mixed solution of two sorts of heterogeneous QDs, called QD_A and QD_B, and a photo-curable
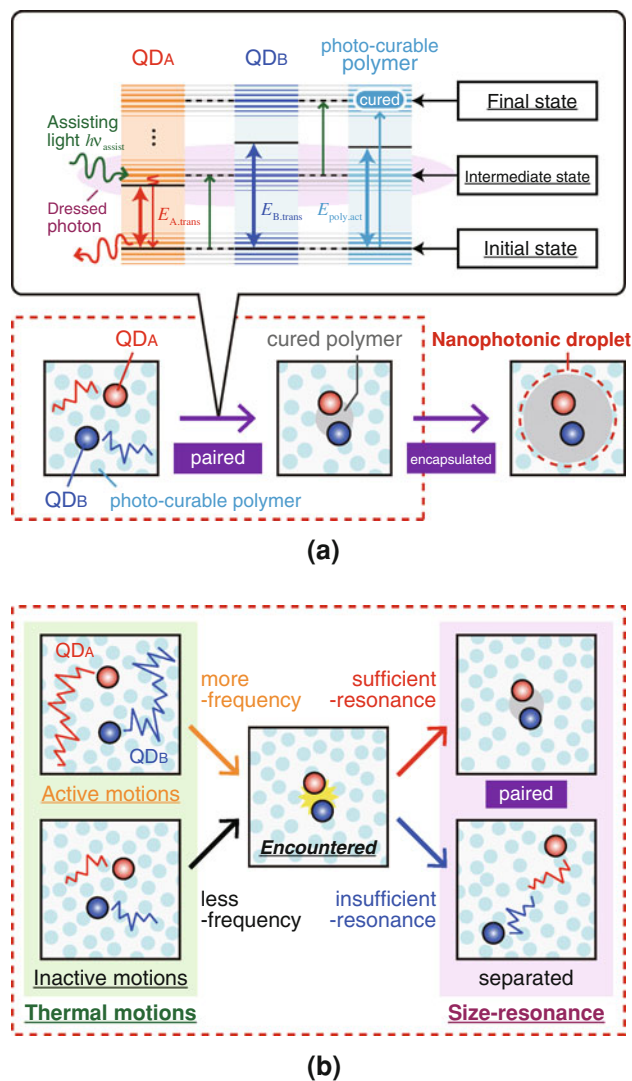
Fig. 1 a Schematic diagram of nanophotonic droplet formation, consisting of pairing and encapsulating processes based on a phonon-assisted photo-curing method. **b** Detailed diagram of the pairing process, considering the effects of velocity-fluctuation and size-resonance between QD_A and QD_B

polymer. In order to induce the sequence, the mixed solution is illuminated by assisting light having photon energy $h\nu_{assist}$. The transition energies of QD_A and QD_B are represented by $E_{A.trans}$ and $E_{B.trans}$, respectively, and the activation energy of the photo-curable polymer is represented by $E_{poly.act}$. The following process is induced only when their energy conditions fulfill $E_{A.trans} < h\nu_{assist} < E_{poly.act} < E_{B.trans}$. If the volume densities of the QDs are low, resulting in the long separation between both QDs, only QD_As spontaneously emit light with the appropriate energy upon absorbing the assisting light. In this case, no physical or chemical reactions occur. However, if the volume densities of the QDs are sufficiently high, resulting in a sufficiently short separation between each other, multistep energy excitation of the photo-

curable polymer occurs due to DPP-mediated optical near-field interactions with neighboring QD_As and QD_Bs, and the photo-curable polymer is subsequently cured. Although there is a subsequent process of encapsulating the coupled QDs by the spontaneous emission of optical energy from the QDs, we focus only on the coupling process in this paper, because the actual electronic transitions involved in the encapsulating process has been described in the authors' previous paper [18].

The detailed coupling process is schematically shown in Fig. 1b. As shown, two factors are considered before and after an encounter, namely, the velocity-fluctuation of QDs for encountering each other and the size-resonance between the encountered QDs, respectively. The former mainly depends on the temperature, i.e., the energy of the fluctuation in the mixed solution. Because higher mobility causes higher frequency of encounter, the temperature of the mixed solution directly affects the pairing process. Then, if the QDs encounter, the size-resonance must govern the efficient induction of the DPP-mediated optical near-field interactions between encountered QDs [19].

3 Experimental formation of nanophotonic droplet

In order to verify the size-resonance in the pairing process, three kinds of CdSe QDs (QD_A) (CdSe_546, CdSe_557, and CdSe_578; Ocean Optics, Inc., *Evidot*) were individually used for coupling with the CdS QDs (QD_B) (CdS_415; NN-Labs, LLC., *Nanocrystals*). The QDs exhibited evidently different emission spectra, as shown in Fig. 2b. A mixed solution of the QD solutions and a UV-curable polymer (Tesk Co., Ltd.; *A1527*) was illuminated assisting light emitted from a 120 mW laser diode having a photon energy of 2.33 eV. Figure 2a shows the relevant energy levels of QDs and UV-curable polymer molecule in the following experiment. These experimental conditions fulfill the previously described energy conditions for inducing the phonon-assisted photo-curing to form nanophotonic droplets. The total amount of mixed solution was limited to 50 μL to maintain spatially uniform illumination by the assisting light. This volume contained about 10^{14} CdSe QDs and about 10^{15} CdS QDs. Under these experimental conditions, the QDs can be assumed to encounter each other at a sufficiently high frequency to induce the phonon-assisted process efficiently.

After 3 h of illumination by the assisting light, the cured substances were extracted from the mixed solution by centrifugation at 10,000 rpm for 5 min. The extracted cured substances, containing a large number of nanophotonic droplets, were dispersed in a toluene solution and uniformly spin-coated on a Si substrate. Figure 3a, b, respectively, show SEM images and microscope emission

(a)

(b)
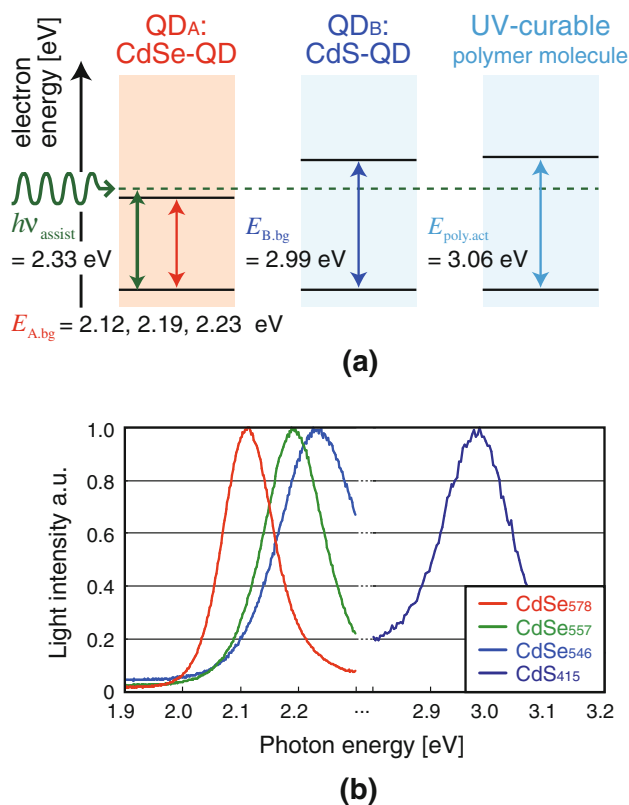
Fig. 2 a Energy diagram of the experimental conditions for forming nanophotonic droplets containing paired CdSe QDs and CdS QDs. To verify the size-dependency, three sorts of CdSe QDs were individually used. **b** Emission spectra of QDs under UV light irradiation
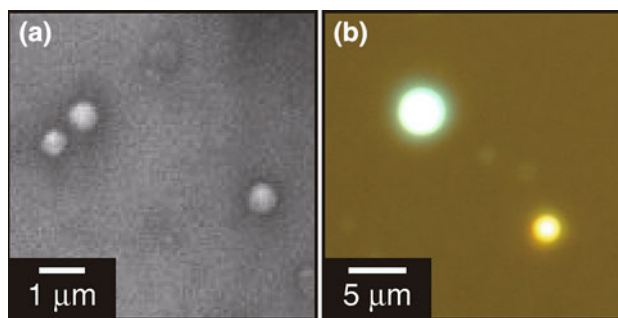

Fig. 3 a SEM images and **b** microscope emission images of formed nanophotonic droplets

images under UV light illumination. As shown, homogeneous-sized spherical nanophotonic droplets were successfully obtained, exhibiting bright emission light spots.

4 Size- and temperature-dependencies in the formation process

The nanophotonic droplet formation process is studied by measuring the temporal evolution of their emission spectra
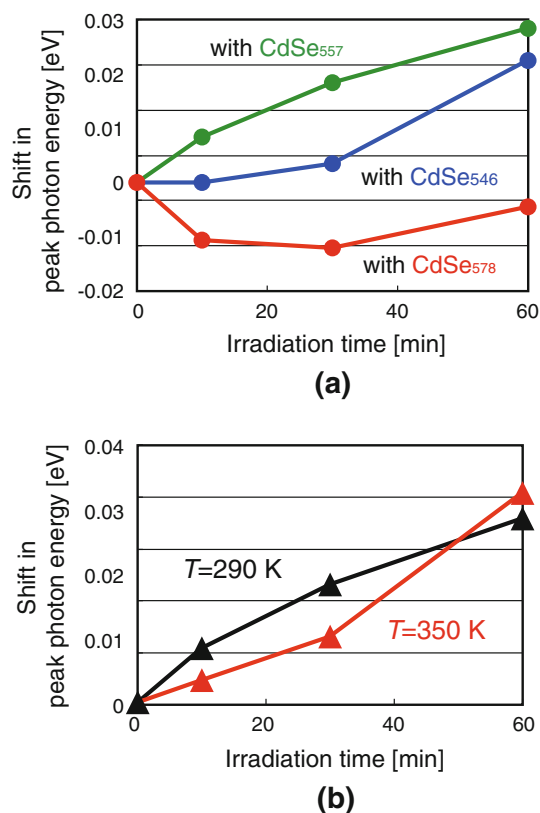
(a)

(b)
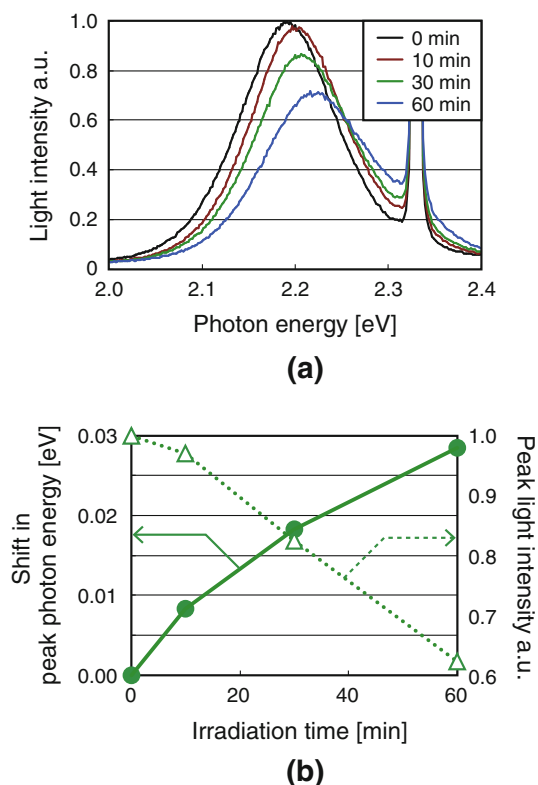
Fig. 4 **a** Experimentally obtained temporal evolution of the emission spectra from CdSe QDs in a mixed solution during illumination by assisting light. **b** Plotted results of the shifted value of the peak photon energy and its light intensity

(a)

(b)

Fig. 5 Temporal evolution of shift in peak photon energy emitted from the mixed solution of CdSe QDs, CdS QDs, and UV-curable polymer during illumination by assisting light **a** using CdSe QDs with various size distributions and **b** with mixed solutions at different temperatures to induce various levels of velocity-fluctuation

while radiating the assisting light. As we previously reported in [19], because each QD preferably make a pair with another QD of similar size due to the size-resonance effect [20], emission from paired CdSe QDs decreases as a result of the energy transfer to its partner of the pairing, i.e., to CdS QD with resonant size. As a result, the peak photon energy of the total emission spectrum from CdSe and CdS necessarily shifts. The magnitude of the shift depends on the sizes of these QDs. Moreover, because only paired QDs are allowed to transfer the irradiated optical energy to the surrounding polymer for its activation, the light intensity of the emission from paired QDs necessarily decreases in the formation process of nanophotonic droplets.

Figure 4a shows the experimentally obtained temporal evolution of the emission spectra from CdSe QDs in a mixed solution of $CdSe_{557}$ QDs, CdS_{415} QDs, and UV-curable polymer during irradiation with assisting light. Their peak photon energies and their emission intensities are plotted as a function of time in Fig. 4b, which monotonously change, as are expected. Here, we focus on the shift of the peak photon energy and describe below.

Figure 5a shows the magnitude of the shift in photon energy during the pairing between CdS_{415} QDs, and $CdSe_{546}$, $CdSe_{557}$, and $CdSe_{578}$ QDs. In this figure, because

average size of the $CdSe_{557}$ QDs is tuned to size-resonant to the CdS_{415} QDs, they showed the steepest gradient of the blue shift in the photon energy. On the other hand, the average sizes of $CdSe_{546}$ and $CdSe_{578}$ are slightly off-resonant to CdS_{415} QDs, resulting in red shift, which is exhibited at an early phase in the coupling process, from 0 to 30 min. The magnitude of such the red shift depends on the degree of off-resonance.

Next, to verify the dependence of the velocity-fluctuation on the temperature during the pairing process, further experiments were performed to measure the temporal evolution of the emission spectra using a hot-water bath. Its temperature, *T*, was fixed to 350 and 290 K, that is, the temperature in the former was 1.2 times that in the latter. Size-resonant $CdSe_{557}$ QDs and CdS_{415} QDs were used for this experiment. Figure 5b shows the observed time variation of the peak photon energy of the emission during irradiation with assisting light. Similarly to the cases of blue circles in Fig. 5a, a lower gradient was observed at an early phase of the variation in the case of $T = 350$ K. Moreover, after this early phase, a steeper gradient was observed, and a larger shift than in the case of $T = 290$ K

is obtained. Such differences are due to increased frequency of encounters driven by higher temperature.

5 Stochastic modeling of the coupling process

In order to numerically model the QD pairing process, we defined a pairing rate and constructed a stochastic model. The pairing rate depends on two factors, the frequency of encounter and the pairing, as schematically shown in Fig. 1b. Thus, our model consists of two stochastic procedures. For the sake of simplicity, one-dimensional coordinate space is considered in the modeling.

As shown by the experiments described above, the pairing rate depends on the size-resonance. It is numerically modeled by considering the size distribution of QD_Bs. Figure 6a shows assumed size distributions of three sorts of QD_Bs, QD_{small}, QD_{medium}, and QD_{large}, which correspond to the actual emission spectra observed in the above experimental demonstrations, as shown in Fig. 2b. Here, we define the allowance size for pairing, $\Delta\phi_{pref}$, which was experimentally estimated to be $3.90 < \Delta\phi_{pref} < 3.98$. At the first step of the numerical trial in our model, the size of QD_B is randomly selected. Then, the following sequence is executed only when the selected size is within the distribution of $\Delta\phi_{pref}$. Otherwise, the trial is terminated and another trial is launched.

The frequency of encounter experimentally depends on the temperature. Here, two one-dimensional coordinates are assumed for its estimation. Each coordinate representing the position of QD randomly fluctuates within an appropriate range until the coordinates of the two QDs crosses, or until a sufficient number of numerical steps is processed. Here, the range of the coordinate fluctuation corresponds to the temperature. Figure 6b shows the calculated temporal evolutions of the coordinate for higher and lower temperature, where the amplitude of the former was on average 1.2 times larger than the latter. This ratio was approximately set based on the difference in velocity-fluctuation due to the temperature in the cases of $T = 350$ and 290 K, which correspond to the experimental conditions in the demonstration described above. In the following, corresponding cases to $T = 350$ and 290 K in the experimental demonstrations are described as high-T and low-T cases, respectively. As shown, the high-T case shows that the QDs encounter within shorter period than the low-T case. After the two QDs successfully encounter, another trial is started selecting other sized QDs. After a sufficient number of iterations, pairing rate of the QDs is calculated as the ratio of the total number of successful encounters to the number of trials.

Based on the above modeling, the dependency of the size-resonance and the temperature on the pairing rate was
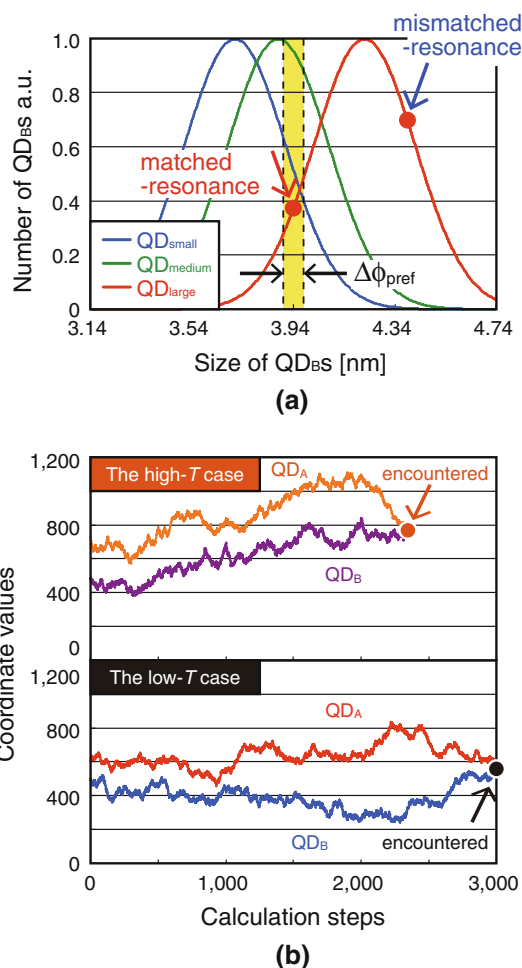
Fig. 6 a Numerically assumed size distributions of QD_Bs in the stochastic model. **b** Comparison of random fluctuations of one-dimensional coordinates between the high-T and low-T cases in the stochastic model

numerically verified. The results are shown in Fig. 7a, b, respectively. As shown, all curves showed monotonous increases of the pairing rate. In particular, in Fig. 7a, the increase with the steepest gradient was found with QD_{medium}, rather than QD_{small} and QD_{large}, agreeing with the previous experimental results in Fig. 5a. Moreover, in Fig. 7b, the pairing rate for the high-T case was higher than for the low-T case agreeing with the experimental results in Fig. 5b.

In our stochastic model, only the frequency of successful pairing between QDs is considered, and subsequent shifts in the peak photon energy of their emission spectra are ignored for the sake of simplicity. This may be one explanation for some of the differences between the experimental and numerical results, especially the red shift in the early phase of the coupling process. Nevertheless, with such approximations in our models, the time-evolving behaviors were in sufficient agreement. The results
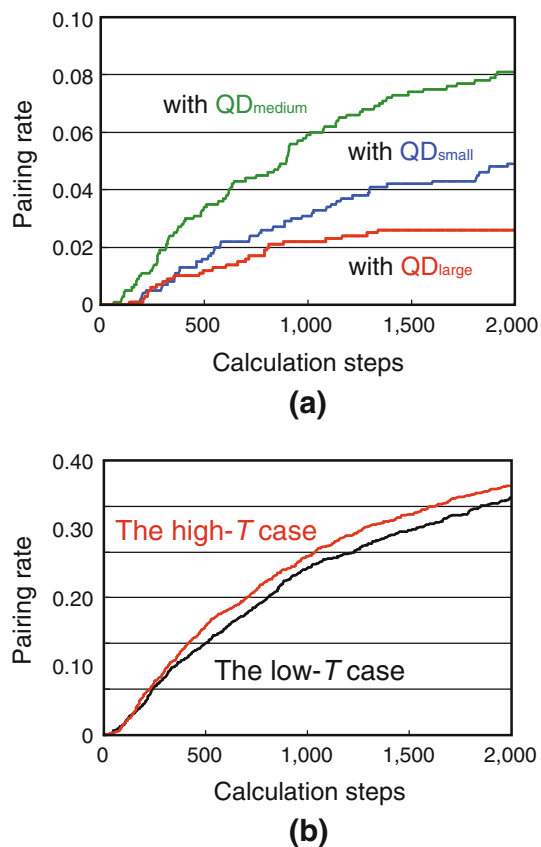
Fig. 7 Numerical verification of dependency of pairing rate on **a** the size difference and **b** the temperature based on the stochastic model

namely, the autonomy of the process and the homogeneity of the products, depend on the size-resonance of DPP interactions and the temperature. In future research, based on the findings described here, it should be possible to assemble nanophotonic droplets that exhibit particular optical properties.

strongly indicate that the autonomy of the process and the homogeneity of the products depend on the size-resonance and the temperature, as we expected.

6 Summary

We have described some experiments demonstrating the formation of nanophotonic droplets consisting of CdSe QDs, CdS QDs, and UV-curable polymer. Temporal evolutions of the emission spectra were experimentally obtained to verify the effects of size-dependency and temperature on the pairing process. To numerically verify the dependency of each factor, a numerical model based on two stochastic procedures was constructed, and temporal evolutions of the QD pairing rate were calculated. Comparison of the experimental and numerical time variations showed sufficient agreement. These results strongly indicate that the characteristics of the phonon-assisted photocuring method for formation of nanophotonic droplets,

References

1. M. Ohtsu, T. Kawazoe, T. Yatsui, M. Naruse, IEEE J. Sel. Top. Quantum Electron **14**, 1404 (2008)
2. T. Kawazoe, K. Kobayashi, S. Sangu, M. Ohtsu, Appl. Phys. Lett. **82**(18), 2957 (2003)
3. S. Yukutake, T. Kawazoe, T. Yatsui, W. Nomura, K. Kitamura, M. Ohtsu, Appl. Phys. B-Lasers Opt. **99**, 415 (2010)
4. H. Fujiwara, T. Kawazoe, M. Ohtsu, Appl. Phys. B-Lasers Opt. **98**, 283 (2010)
5. T. Kawazoe, M.A. Mueed, M. Ohtsu, Appl. Phys. B-Lasers Opt. **104**, 747 (2011)
6. K. Kitamura, T. Kawazoe, M. Ohtsu, Appl. Phys. B-Lasers Opt. **107**, 293 (2012)
7. T. Kawazoe, K. Kobayashi, M. Ohtsu, Appl. Phys. Lett. **86**(10), 103102 (2005)
8. W. Nomura, T. Yatsui, T. Kawazoe, M. Ohtsu, J. Nanophotonics **1**, 011591 (2007)
9. M. Naruse, K. Leibnitz, F. Peper, N. Tate, W. Nomura, T. Kawazoe, M. Murata, M. Ohtsu, Nano Commun. Netw. **2**(4), 189 (2011)
10. T. Kawazoe, M. Ohtsu, S. Aso, Y. Sawado, Y. Hosoda, K. Yoshizawa, K. Akahane, N. Yamamoto, M. Naruse, Appl. Phys. B **103**(3), 537 (2011)
11. B.Q. Wei, R. Vajtai, Y. Jung, J. Ward, R. Zhang, G. Ramanath, P.M. Ajayan, Nature **416**, 495 (2002)
12. B.A. Parviz, D. Ryan, G.M. Whitesides, IEEE Trans. Adv. Packaging **26**, 233 (2003)
13. Y.I. Mazur, Z.M. Wang, G.G. Tarasov, M. Xiao, G.J. Salamo, J.W. Tomm, V. Talalaev, H. Kissel, Appl. Phys. Lett. **86**, 063102 (2005)
14. M.P. Stoykovich, M. Müller, S. Ouk Kim, H.H. Solak, E.W. Edwards, J.J. de Pablo, P.F. Nealey, Science **308**, 1442 (2005)
15. T. Yatsui, K. Hirata, W. Nomura, Y. Tabata, M. Ohtsu, Appl. Phys. B **93**(5), 55 (2008)
16. Y. Liu, T. Morishima, T. Yatsui, T. Kawazoe, M. Ohtsu, Nanotechnology **22**(21), 215605 (2011)
17. T. Kawazoe, M.A. Mueed, M. Ohtsu, Appl. Phys. B **104**(4), 747 (2011)
18. N. Tate, Y. Liu, T. Kawazoe, M. Naruse, T. Yatsui, M. Ohtsu, Appl. Phys. B-Lasers Opt. **110**, 39 (2013)
19. N. Tate, Y. Liu, T. Kawazoe, M. Naruse, T. Yatsui, M. Ohtsu, Appl. Phys. B-Lasers Opt. **110**, 293 (2013)
20. S. Sangu, K. Kobayashi, M. Ohtsu, J. Microsc. **202**, 279 (2001)